Digest Journal of Nanomaterials and Biostructures Vol. 19, No. 4, October-December 2024, p. 1395-1406

Facile synthesis of nanoflowers of immobilized enzyme using layered rare earth hydroxides as carriers and their application for detection of H_2O_2 and phenol

X. Y. Liang[a,#], K. Ren[a,c,#], X. L. Wu[a,b,*]
[a]*Guangxi Key Laboratory of Optical and Electronic Materials and Devices, Guilin University of Technology, Guilin 541004, China*
[b]*Provincial Ministry Collaborative Innovation Center for Non-ferrous Metal Mineral Exploration and Efficient Resource Utilization, Guilin 541004, China*
[c]*School of Molecular Medicine, Hangzhou Institute for Advanced Study, University of Chinese Academy of Sciences, Hangzhou, 310024, China*

This study reports a simple method for synthesizing the nanoflower-immobilized enzyme (LYH-HRP) using horseradish peroxidase (HRP) as the bioenzyme and layered yttrium hydroxide (LYH) as the inorganic carrier. Utilizing the structural advantage of LYH and the catalytic properties of HRP, a nanoflower-based colorimetric platform was newly designed and applied for sensitively detecting H_2O_2 and phenol with a detection time of as fast as 5 min. The limits of detection (LODs) for H_2O_2 and phenol are as low as 0.046 μM and 0.778 μM, respectively. The activity and stability tests showed that the activity of LYH-HRP was 1.52 times that of free HRP, and it maintained 75% of the initial activity after 60 days.

(Received April 6, 2024; Accepted October 4, 2024)

Keywords: Layered yttrium hydroxide, Horseradish peroxidase, Immobilized enzyme

1. Introduction

Enzymes are natural catalysts that exist extensively in nature. They have high catalytic activity and biocompatibility [1]. Enzyme catalysis exhibits high catalytic activity, selectivity, peculiarity, and environmental friendliness under mild conditions (25 ℃, 1 atm, and neutral pH) [2]. Enzymes increase rates of chemical reactions without altering or consuming the reaction itself. They also raise the reaction rates without affecting the equilibrium of the reactants and products [3]. However, free enzymes present shortcomings such as poor stability, easy deactivation and difficult recovery during use [4]. This problem was solved by the introduction of immobilized enzymes.

Immobilized enzymes may be defined as the physical or chemical binding of a free enzyme to a carrier, which "strengthen" the surface of the enzyme, thereby enhancing the stability of the enzyme. In previous studies, many materials such as polymer semiconductors, metal-organic frameworks, silicon microspheres and nanostructured support materials have been used as carriers

*Corresponding author: wuxiaoli@glut.edu.cn
# These authors contributed equally to this work
https://doi.org/10.15251/DJNB.2024.194.1395

for immobilizing free enzymes [5-7]. These materials immobilize the free enzyme by hierarchical assembly, cross-linking and covalent binding [8-11]. Although immobilization produces enzyme catalysts with higher stability and recoverability to environmental alterations, most enzymes lose their biocatalytic properties during conventional immobilization due to blocked enzyme catalytic sites, limited flexibility, and resistance to mass transfer between enzyme molecules and substrates [12, 13].

In 2012, Gejun et al. synthesized a series of "enzyme-copper phosphate" hybrid nanoflower immobilized enzymes by co-precipitation of copper sulfate in a phosphate buffer solution containing protease (pH ~7 and 25 ℃) [14]. These immobilized enzymes enhanced the stability and improved their catalytic activity significantly. For example, the catalytic activity of immobilized laccase was 6.5 and 4.5 times higher than that of the free enzyme in the experiments for the oxidation of catecholamine and clove-pyridazine, respectively. At the same time, the catalytic activity of carbonic anhydrase for carbon dioxide hydration reaction is 2.6 times higher than that of the free enzyme. An important reason for the significant enhancement of catalytic activity is that the flower-like morphology of the immobilized enzyme has a high specific surface area and surface energy, resulting in the reduction of the resistance to mass transfer between enzyme-substrate products. Nanoflower-immobilized enzymes have higher activity and better stability than free enzymes and therefore have broader application prospects [15-17]. In addition to the nano-flower immobilized enzyme with copper phosphate as the carrier, Zeng Jie's group has developed the "Amylase-$CaHPO_4$" nano-flower immobilized enzyme with calcium hydrogen phosphate as the carrier. The catalytic activity of the enzyme increased significantly due to favorable conformational changes of the enzyme molecule during the immobilization process. However, the inorganic carriers for the nanoflower-like immobilized enzymes were limited to phosphate systems in the previous studies [18-22].

$RE_2(OH)_5NO_3 \cdot nH_2O$ Layered rare-earth hydroxides (LRHs) are emerging layered compounds [23]. The structure of LRHs consists of positively charged $[RE_2(OH)_5 \cdot nH_2O]^+$ host layers and interlayer NO_3^-. As the $[RE_2(OH)_5 \cdot nH_2O]^+$ host layer is a close-packed low-energy plane, the LRH crystal preferentially grows along the *ab* plane, which leads to the nanoflower-like morphology at room temperature and precisely meets the requirement of the ideal carrier. HRP is considered a versatile enzyme and has drawn special attention due to its catalytic capabilities at various temperatures, pH values, and pollution concentrations. Herein, we developed a novel nanoflower-like immobilized enzyme with LRH as the carrier and HRP as an enzyme to detect hydrogen peroxide (H_2O_2) and phenols.

2. Material and methods

2.1. Materials and instruments

The $Y(NO_3)_3 \cdot nH_2O$ (purity 99.9%) was purchased from Cabosens Chemical Technology Co. Ammonium nitrate was purchased from Guangzhou Chemical Reagent Factory, ammonia (96% purity) from Xilong Technology Co. Horseradish peroxidase was obtained from Sigma-Aldrich Trading Co.

Physical and chemical of the immobilized enzyme were characterized using XRD(Panaco, X'Pert PRO), SEM(Hitachi, S-4800), FT-IR(Thermo Fisher Scientific, Nexus 470) and TGA(TA

Instruments, Q500). Hydrogen peroxide and phenol were determined using a UV spectrophotometer(Shimadzu, UV-3600).

2.2. Synthesis of LYH-HRP

$Y(NO_3)_3$ (1.915 g) and NH_4NO_3 (2.001 g) were dissolved in 50 mL deionized water to form solution A. HRP (0.1-2 mg/mL) was dispersed in solution A to produce solution B. After 30 minutes of stirring, 25 wt.% ammonium hydroxide solution was added to solution B until the pH value was around 7. The resulting suspension was magnetically stirred for 30 minutes, then washed with deionized water and dried to obtain a white powder.

2.3. Determination of encapsulation efficiency

The Bradford method evaluated encapsulation efficacy, which is defined as the ratio of the enzyme immobilized by the carrier material to the total amount of enzyme. Immobilized enzymes and free enzymes prepared at different concentrations of HRP were reacted with Komas Brilliant Blue solution. The absorbance of the supernatant was measured at 595 nm to calculate the solid loading rate of biological enzymes. The expressions (1) were:

$$EN\%=(1-C_f/C_t)\times 100\% \quad (1)$$

In the above equation, C_f represents the number of free enzymes; C_t represents the total number of enzymes.

2.4. Test of enzyme activity

According to the national standard GB/T 32131-2015, horseradish peroxidase can rapidly catalyze the oxidation of guaiacol by hydrogen peroxide to produce brown tetra-o-methoxyphenol. The change of absorbance at 436 nm was used to calculate enzyme activity. The enzyme activity assay was completed at least two parallel experiments at a time and its enzyme activity was estimated by this formula:

$$U=(\Delta A\times 3.0\times 4\times D)/(25.5\times 1\times 0.05\times 2)\times 1000 \quad (2)$$

In the above equation, U represents the enzyme activity of the liquid sample in milliliters (mL); ΔA represents the value of the change in absorbance of the sample; 3.0 represents the total volume of the reaction reagent in milliliters (mL); 4 means the coefficient of conversion of the amount of tetra-o-anisole to hydrogen peroxide; D represents the dilution multiple; and 25.5 represents the molar extinction coefficient of tetra-o-anisole in L/(mol·cm).

2.5. Test of catalytic activity

The catalytic activity of LYH-HRP immobilized enzyme was tested based on the color development reaction of 3,3′,5,5′-tetramethylbenzidine (TMB). The reaction equation is shown in Figure 2. In a PBS buffer (pH=5) including 0.1 mmol/L TMB and 20 mmol/L H_2O_2, the product TMB_{ox} generated by HRP-Catalysed oxidation of TMB had absorption peaks at 370 nm and 652 nm [24]. Based on the above reaction, UV spectroscopy recorded the absorbance value of the peak at 652 nm as a function of time, revealing reaction progression in the catalyst's performance.

2.6. Test of stability

Storage stability is a critical evaluation criterion for enzymes. We evaluated the stability of LYH-HRP immobilized and free HRP enzymes by leaving them at room temperature for 1, 2, 5, 10, 25, 45 and 60 days, respectively, and then conducting activity tests.

2.7. Detection of H_2O_2 and phenol

Based on the TMB chromogenic reaction catalyzed by the LYH-HRP, H_2O_2 in the system was detected by monitoring the absorbance of TMB_{ox} located at 652 nm. 20 μL of a suspension of LYH-HRP was added to 2 mL of PBS (25 mmol/L, pH=5.0) including 0.1 mmol/L TMB and different concentrations of H_2O_2 at room temperature. The reaction was carried out in buffer solution and the absorbance at 652 nm (A_{652}) was detected after the reaction reached equilibrium (3 min).

Colorimetric detection of phenolic compounds via reactions between 4-aminoantipyrine and phenol. A suspension of 20 μL LYH-HRP was mixed with 2 mL of PBS (25 mmol/L, pH=7.4) buffer solution including 4 mmol/L 4-AAP, 10 mmol/L H_2O_2, and different concentrations of phenol, and detected the absorbance at 505 nm(A_{505}) after the reaction had reached equilibrium (within 5 min).

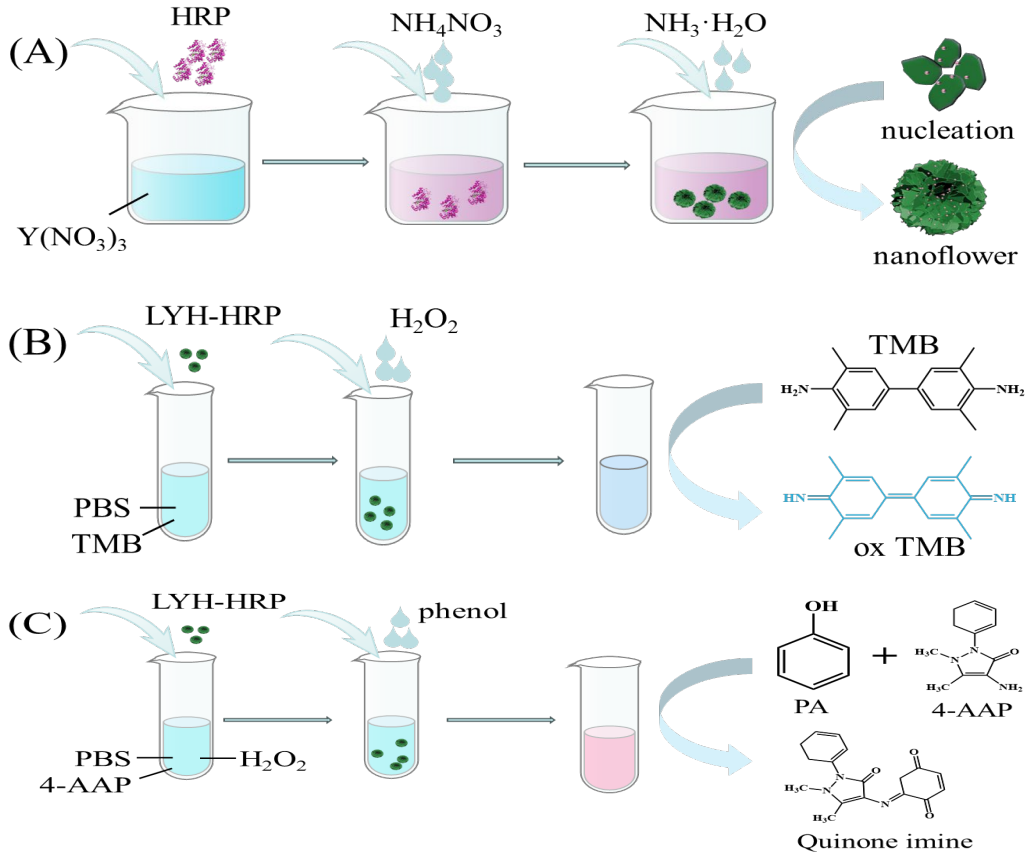

Fig. 1. Synthesis scheme for LYH-HRP nanoflowers (a); a nanoflower-based colorimetric platform for detection of H_2O_2 (b) and phenol (c).

3. Results and discussions

3.1. Encapsulation efficiency and activity of LYH-HRP

Figure 1a demonstrates the typical synthesis process of LYH-HRP nanoflowers. The solidification rate of LYH-HRP immobilized enzyme prepared at different HRP concentrations was determined using the Bradford method. As shown in Table 1, the solidification rate of LYH-HRP enzyme prepared with different concentrations of HRP is over 80%. Enzyme solidification exhibits an initial upward trend followed by a decrease with increasing in HRP concentration. When the concentration of HRP is 0.5 mg/mL, the enzyme solidification achieves a peak of 98.11% indicating that LYH has good biocompatibility. The enzyme activity determination of diverse free HRP and LYH-HRP immobilized enzymes at varied concentrations is delineated in Table 2. When the content of HRP is within the range of 0.1-0.2 mg/mL, LYH-HRP immobilized enzymes demonstrate decreased activity compared to their equivalent free counterparts. However, LYH-HRP immobilized enzymes exhibit enhanced activity when the concentration of HRP is 0.5 mg/mL, which is 1.52 times that of free HRP. From this, it can be judged that LYH as an inorganic carrier promotes the enzyme activity at a suitable ratio with HRP.

Table 1. Results of enzyme solidification.

number	Theoretical concentration(mg/mL)	Actual concentration (mg/mL)	Absorbance (595 nm)	The supernatant solubility(mg/mL)	The supernatant absorbance (595 nm)	Encapsulation efficiency (%)
Sample1	0.1	0.091	0.0716	0.0437	0.0067	90.64
Sample2	0.2	0.2049	0.2017	0.0387	0.0043	97.87
Sample3	0.5	0.4962	0.2868	0.1443	0.0054	98.12
Sample4	1	1.0486	0.6041	0.0341	0.0271	95.51
Sample5	2	1.8766	1.4250	0.8043	0.1791	87.43

Table 2. Results of enzyme activity determination.

Sample	Enzyme activity (U/mg)
HRP (0.1 mg/mL)	11764
HRP (0.2 mg/mL)	13176
HRP (0.5 mg/mL)	14117
LYH-HRP (Sample 1)	6117
LYH-HRP (Sample 2)	7058
LYH-HRP (Sample 3)	21405

3.2 Characteristics of immobilized enzymes

As depicted in Figure 2a, (002), (004), and (220) are the characteristic diffractions of LYH, where the (220) and (00*l*) diffractions signify the host layer structural characteristics and its alignment in the c-axis of crystal structure, respectively. Compared with LYH, the (220) peak position of LYH-HRP remains unaltered, implying an unmodified host layer structure. However, $d_{(002)}$ increases from 0.906 nm to 0.917 nm, indicating that the enzyme has been inserted into the interlayer (Figure 2b). The FT-IR spectra (Figure 2c) show that both LYH and LYH-HRP exhibit characteristic absorption peaks of free NO_3^- at 1384 cm^{-1}, stretch vibration peaks of the hydroxyl group at 3600 cm^{-1}, O-H stretch vibration (ν_1 and ν_3) peaks of the water of crystallization near 3381 cm^{-1}, and absorption peaks of the hydroxyl group at 3500-3750 cm^{-1}. For the LYH-HRP, in addition to the absorption peaks of LYH, the absorption bands of protein amide I and II are also displayed at 1657 cm^{-1} and 1548 cm^{-1}, respectively [24, 25]. The TG analysis (Figure 2d) reveals that LYH-HRP has a greater total weight loss than LYH, confirming that HRP is involoved in the thermal decomposition. Notably, the weight loss in the first stage of thermal decomposition of LYH-HRP is comparable to that of LYH, suggesting that the bio-enzyme is immobilized within LYH without destroying its host layer, being inserted only between the host layers. Figure 2e-2f show the morphology of LYH and LYH-HRP, respectively. The LYH-HRP inherits the flower-like morphology of LYH, but the size of the nanosheets has been decreased. This may be ascribed to the adsorption of HRP on the initial crystal nucleus and thus significantly confines the lateral growth.

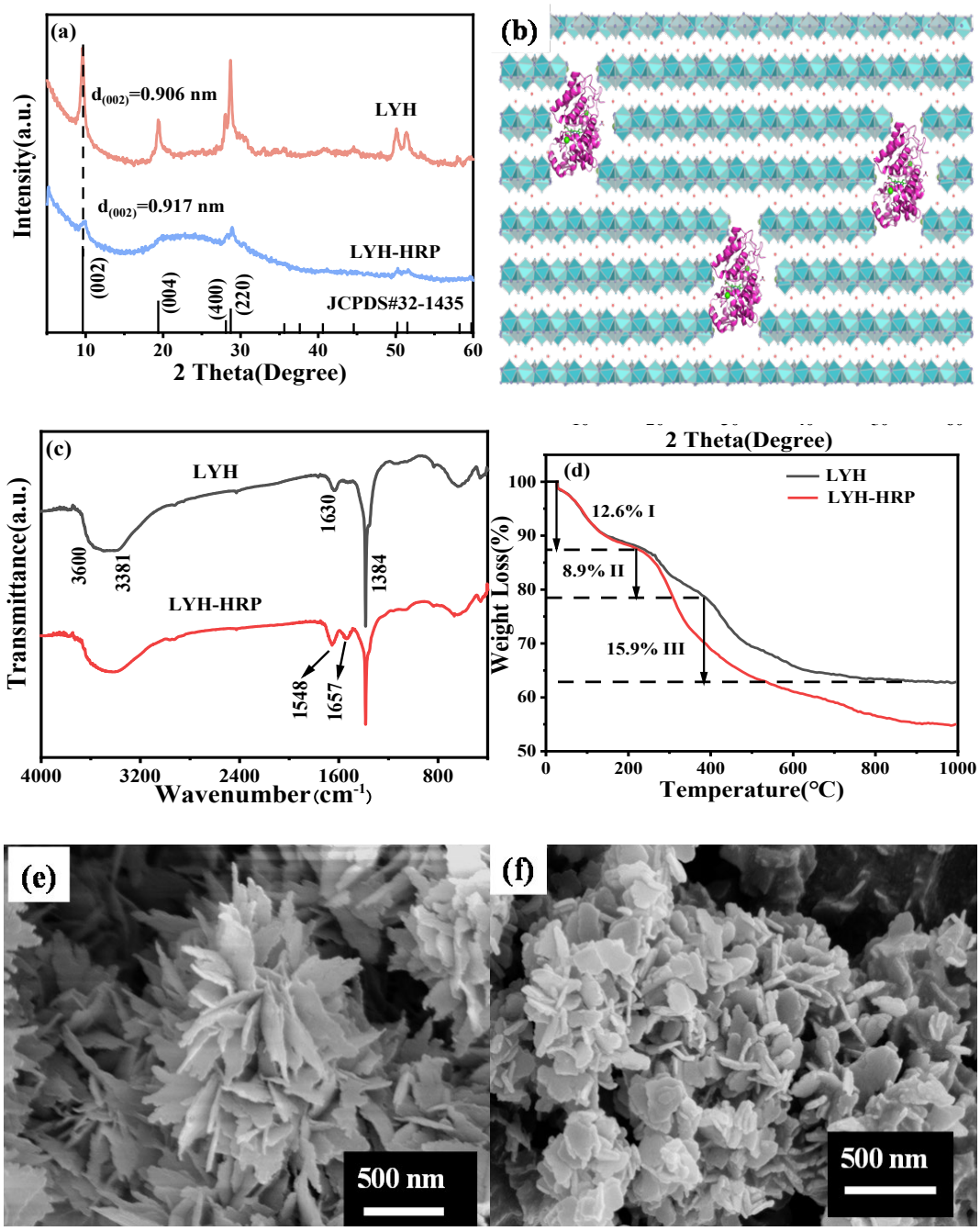

Fig. 2. XRD patterns (a); structure schematic of LYH-HRP (b); FT-IR spectra (c); TG curves (d); SEM images (e, f) for LYH and LYH-HRP.

3.3. Catalytic activity detection of immobilized enzymes

The catalytic performance of the immobilized enzyme was carried out based on the TMB chromogenic reaction. From the UV-vis absorption spectra in Figure 3a, the absorption peaks at 400 nm and 285 nm are ascribed to the absorption of HRP and TMB, respectively. The reaction product Benzidine oxide (TMB_{ox}) exhibits absorption bands at 370 nm and 652 nm, respectively. The kinetics of these oxidation reactions with free HRP and LYH-HRP are monitored by the changes in absorbance at 652 nm (Figure 3b). For the free HRP reaction system, the absorbance

value of the absorption peak at 652 nm increases slowly and reaches a platform after 1200 s. Conversely, the absorbance value of TMB_{ox} achieves a platform within 200 seconds for the LYH-HRP system. The results indicate that the catalytic activity of LYH-HRP is higher than that of free HRP. This can be attributed to the high surface area of the nanoflower-like structured LYH-HRP, which makes the substrate more accessible to the active site and enhances its catalysis activity.

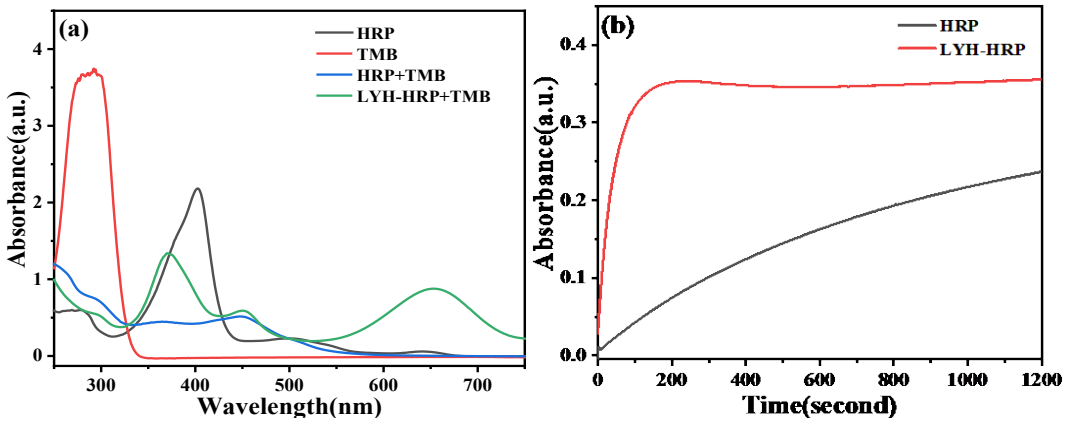

Fig. 3. UV-vis absorbance spectra of HRP, TMB, and mixture of TMB and product catalyzed by free HRP and LYH-HRP, respectively (a); catalytic kinetics of the oxidization of TMB by free HRP and LYH-HRP (b).

3.4. Stability of immobilized enzymes

Stability is another important evaluation criterion for enzymes. The stabilities of LYH-HRP and free HRP were evaluated by tracking their activity after post-prolonged storage under ambient room conditions. Refer to Figure 4, 50% of the activity is lost for the free HRP after 10 days, while LYH-HRP maintains 90% of the initial activity. After 60 days, LYH-HRP still maintains more than 75% of the initial activity, while the free HRP has less than 20% of the activity. It can be seen that LRH as a carrier can greatly improve the stability of HRP.

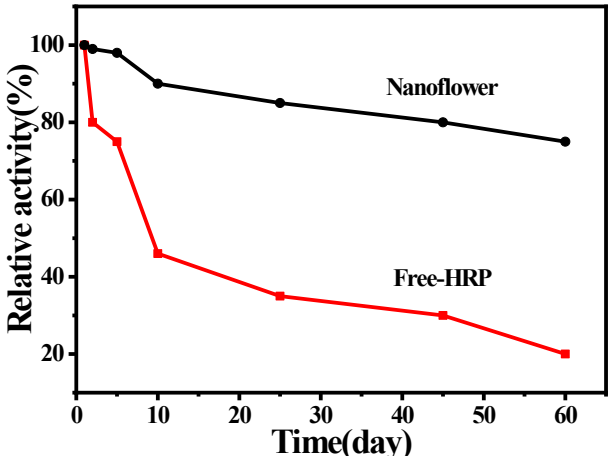

Fig. 4. Room-temperature stability of immobilized versus free HRP over the long term.

3.5. Detection of H_2O_2

To assess the quantification of H_2O_2, as illustrated in Figure 3, different amounts of H_2O_2 (1-20 μM) were introduced into a preprepared PBS solution (25 mM, pH=5.0) containing LYH-HRP and TMB at room temperature. It can be seen that the oxidation reaction is accomplished within 5 minutes, which indicates the excellent catalytic activity of the LYH-HRP. We detected the content of H_2O_2 by tracking the absorbance values of TMB_{ox} at 652 nm. Figure 5a shows that the values of absorbance peak at 652 nm increases linearly with the increase of the H_2O_2 concentration. As shown in Figure 5b, one linear regression is established between A_{652} and the H_2O_2 content within a concentration spectrum spanning 0-20 μM (R^2=0.99915), with a limit of detection (LOD) of 0.046 μM (LOD=3σ/K) [26].

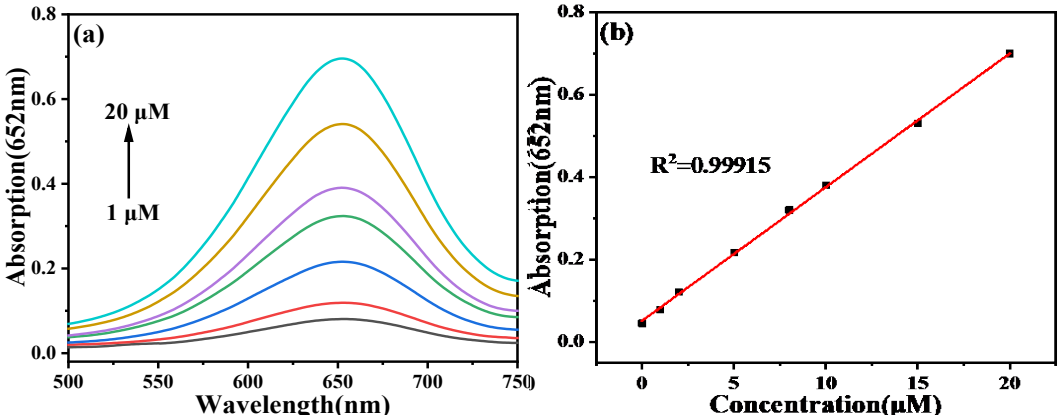

Fig. 5. UV-vis absorbance spectra of TMB_{ox} in the existence of LYH-HRP and various H_2O_2 concentrations (a); a plot of A_{652} versus H_2O_2 concentration (b)

3.6. Detection of phenol

Figure 1c shows a visual detection method for phenol; where different concentrations of phenol were introduced into PBS solution (25 mM, pH=7.4) including the LYH-HRP, H_2O_2 and 4-Aminoantipyrine (4-AAP) at room temperature. The content of phenol in the system is detected by testing the absorbance values at 505 nm(A_{505}) of the product quinone imine. As the amount of phenol in the system gradually increases, the perceivable color gradually enhances (Figure 6a). Referring to Figure 6b, A_{505} increases linearly with increasing phenol concentration in the range of 0-200 μM, with a limit of detection (LOD) is 0.778 μM (LOD=3σ/K) [26].

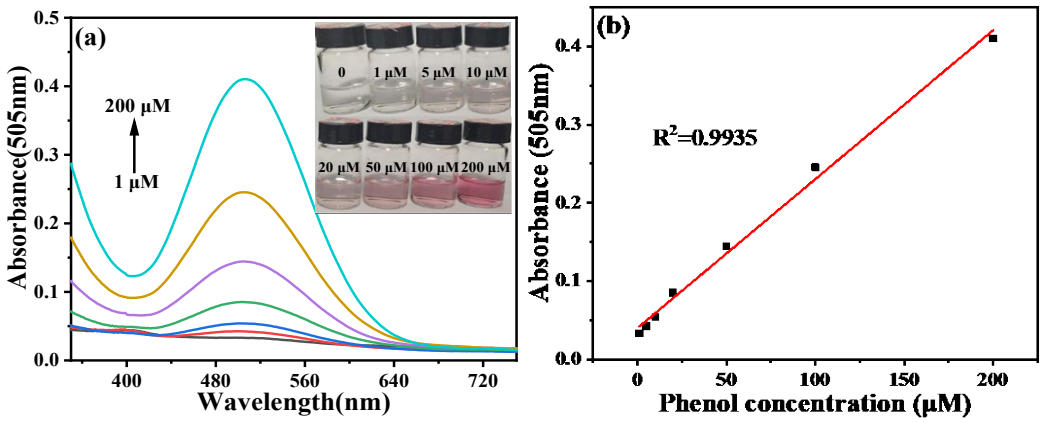

Fig. 6. UV-vis absorbance of Quinone imine in the existence of LYH-HRP and various phenol concentrations (a) and plot of A_{505} versus phenol concentration (b). The inset in (a) is the hue change of the reaction solutions.

4. Conclusions

The LYH-HRP immobilized enzyme was prepared by co-precipitation and systematically evaluated for its activity, stability, and catalytic activity, which was applied to detect H_2O_2 and phenol. A 98.11% encapsulation efficiency was achieved using LYH as the carrier with 0.5 mg/mL HRP. This showed an activity enhancement of 1.52 times that of free HRP, with superior stability retaining 75% of the activity after 60 days at room temperature. In addition, LYH-HRP optimized the TMB catalytic reaction, and the equilibrium reaction time was significantly diminished to facilitate the rapid detection of H_2O_2 and phenol, and the limit of detection (LOD) for H_2O_2 and phenol was 0.046 μM and 0.778 μM, respectively.

Acknowledgments

This work was supported by the National Natural Science Foundation of China (52062011), the Natural Science Foundation of Guangxi Zhuang Autonomous Region (2018GXNSFAA050011), and an independent research project of Guangxi Key Laboratory of Optoelectronic Materials and Devices (20AA-2).

References

[1] R.A. Sheldon, S.v. Pelt, Chemical Society Reviews 42 (15), 6223-6235 (2013); https://doi.org/10.1039/C3CS60075K

[2] D.-M. Liu, J. Chen, Y.-P. Shi, TrAC Trends in Analytical Chemistry 102, 332-342 (2018); https://doi.org/10.1016/j.trac.2018.03.011

[3] N.R. Mohamad, N.H.C. Marzuki, N.A. Buang, F. Huyop, R.A. Wahab, Biotechnol

Biotechnol Equip 29 (2), 205-220 (2016); https://doi.org/10.1080/13102818.2015.1008192

[4] C. Altinkaynak, S. Tavlasoglu, N. Ozdemir, I. Ocsoy, Enzyme Microb Technol 93-94, 105-112 (2016); https://doi.org/10.1016/j.enzmictec.2016.06.011

[5] X. Lian, Y. Fang, E. Joseph, Q. Wang, J. Li, S. Banerjee, C. Lollar, X. Wang, H.C. Zhou, Chem Soc Rev 46 (11), 3386-3401 (2017); https://doi.org/10.1039/C7CS00058H

[6] K. Koeller, C. Wong, Nature 409 (6817), 232-240 (2001); https://doi.org/10.1038/35051706

[7] I. Migneault, C. Dartiguenave, J. Vinh, M.J. Bertrand, K.C. Waldron, Electrophoresis 25 (9), 1367-1378 (2004); https://doi.org/10.1002/elps.200305861

[8] X. Chen, S. Xue, Y. Lin, J. Luo, L. Kong, Anal Chim Acta 1099, 94-102 (2020); https://doi.org/10.1016/j.aca.2019.11.042

[9] E. Moreno-Reyes, J.M. Goddard, ACS Food Science & Technology 1 (3), 304-309 (2021); https://doi.org/10.1021/acsfoodscitech.1c00015

[10] M. Babaki, M. Yousefi, Z. Habibi, J. Brask, M. Mohammadi, Biochemical Engineering Journal 101, 23-31 (2015); https://doi.org/10.1016/j.bej.2015.04.020

[11] X. Qiu, X. Xiang, T. Liu, H. Huang, Y. Hu, Process Biochemistry 95, 47-54 (2020); https://doi.org/10.1016/j.procbio.2020.05.007

[12] M.C.P. Gonçalves, T.G. Kieckbusch, R.F. Perna, J.T. Fujimoto, S.A.V. Morales, J.P. Romanelli, Process Biochemistry 76, 95-110 (2019); https://doi.org/10.1016/j.procbio.2018.09.016

[13] U. Hanefeld, L. Cao, E. Magner, Chem Soc Rev 42 (15), 6211-6212 (2013); https://doi.org/10.1039/c3cs90042h

[14] J. Ge, J. Lei, R.N. Zare, Nat Nanotechnol 7 (7), 428-432 (2012); https://doi.org/10.1038/nnano.2012.80

[15] K. Wu, Y. Zhang, Q. Sun, Y. Chai, Q. He, X. Zhou, X. He, H. Ji, Enzyme Microb Technol 131, 109386 (2019); https://doi.org/10.1016/j.enzmictec.2019.109386

[16] T. Peng, J. Wang, S. Zhao, S. Xie, K. Yao, P. Zheng, S. Wang, Y. Ke, H. Jiang, Mikrochim Acta 185 (8), 366 (2018); https://doi.org/10.1007/s00604-018-2889-0

[17] M. Zhang, M. Chen, Y. Liu, Y. Wang, J. Tang, Materials Letters 243, 9-12 (2019); https://doi.org/10.1016/j.matlet.2019.01.157

[18] M. Kiani, S. Mojtabavi, H. Jafari-Nodoushan, S.R. Tabib, N. Hassannejad, M.A. Faramarzi, Int J Biol Macromol 204, 520-531 (2022); https://doi.org/10.1016/j.ijbiomac.2022.02.023

[19] I. Ocsoy, E. Dogru, S. Usta, Enzyme Microb Technol 75-76, 25-29 (2015); https://doi.org/10.1016/j.enzmictec.2015.04.010

[20] L.-B. Wang, Y.-C. Wang, R. He, A. Zhuang, X. Wang, J. Zeng, J.G. Hou, Journal of the American Chemical Society 135 (14), 1272-1275 (2013); https://doi.org/10.1021/ja3120136

[21] J.C. Munyemana, H. He, S. Ding, J. Yin, P. Xi, J. Xiao, RSC Adv 8 (5), 2708-2713 (2018); https://doi.org/10.1039/C7RA12628J

[22] L. Zheng, Y. Sun, J. Wang, H. Huang, X. Geng, Y. Tong, Z. Wang, Catalysts 8 (10), (2018); https://doi.org/10.3390/catal8100468

[23] F. Gandara, J. Perles, N. Snejko, M. Iglesias, B. Gomez-Lor, E. Gutierrez-Puebla, M.A. Monge, Angew Chem Int Ed Engl 45 (47), 7998-8001 (2006); https://doi.org/10.1002/anie.200602502

[24] M. Wang, W.-J. Bao, J. Wang, K. Wang, J.-J. Xu, H.-Y. Chen, X.-H. Xia, Scientific Reports 4, (2014); https://doi.org/10.1038/srep06606

[25] Z. Lin, Y. Xiao, L. Wang, Y. Yin, J. Zheng, H. Yang, G. Chen, RSC Advances 4

(27), 13888-13891 (2014); https://doi.org/10.1039/C4RA00268G
[26] J. Chai, L. Yuan, S. Wang, T. Li, M. Wu, Z. Huang, H. Yin, New Journal of Chemistry 46 (25), 12372-12380 (2022); https://doi.org/10.1039/D2NJ01981G